Ag/AgBr/TiO_2 Visible Light Photocatalyst for Destruction of Azodyes and Bacteria

Chun Hu,* Yongqing Lan, Jiuhui Qu,* Xuexiang Hu, and Aimin Wang

State Key Laboratory of Environmental Aquatic Chemistry, Research Center for Eco-Environmental Sciences, Chinese Academy of Sciences, Beijing, 100085, P. R. China

Received: November 8, 2005; In Final Form: December 13, 2005

Ag/AgBr/TiO_2 was prepared by the deposition−precipitation method and was found to be a novel visible light driven photocatalyst. The catalyst showed high efficiency for the degradation of nonbiodegradable azodyes and the killing of *Escherichia coli* under visible light irradiation ($\lambda > 420$ nm). The catalyst activity was maintained effectively after successive cyclic experiments under UV or visible light irradiation without the destruction of AgBr. On the basis of the characterization of X-ray diffraction, X-ray photoelectron spectroscopy, and Auger electron spectroscopy, the surface Ag species mainly exist as Ag^0 in the structure of all samples before and after reaction, and Ag^0 species scavenged h_{VB}^+ and then trapped e_{CB}^- in the process of photocatalytic reaction, inhibiting the decomposition of AgBr. The studies of ESR and H_2O_2 formation revealed that $^{\bullet}OH$ and $O_2^{\bullet-}$ were formed in visible light irradiated aqueous Ag/AgBr/TiO_2 suspension, while there was no reactive oxygen species in the visible light irradiated Ag^0/TiO_2 system. The results indicate that AgBr is the main photoactive species for the destruction of azodyes and bacteria under visible light. In addition, the bactericidal efficiency and killing mechanism of Ag/AgBr/TiO_2 under visible light irradiation are illustrated and discussed.

1. Introduction

TiO_2 photocatalysis has been investigated extensively for the killing of bacteria and degradation of different pollutants and demonstrated to be a technically viable cleanup process.[1−5] The main drawbacks of low quantum yields and the lack of visible light utilization, however, hinder its practical application. To handle these problems, numerous studies have recently been performed to enhance the photocatalytic efficiency and visible light utilization of TiO_2, which include impurity doping,[6−9] metallization,[10−15] and sensitization.[16,17]According to these published works, the deposition of the metal on visible light catalysts highly improved its photoefficiency through the Schottky barrier CB electron trapping and consequent longer electron−hole pair lifetimes.[10,13] The results suggest that the development of better visible light photocatalysts depends on visible light photoresponse and highly effective interfacial charge transfer.

Silver halides are well-known as photosensitive materials and widely employed as source materials in photographic films. In the photographic process, the silver halides absorb a photon and liberate an electron and a positive hole. The electron will combine with a mobile interstitial silver ion, leading to separation of a silver atom. Upon repeated absorption of photons, a cluster of silver atoms can be formed ultimately. This displays that silver halides are unstable under irradiation of light. Because of these properties, silver halides have not been studied so much in photocatalytic reactions. Recently, a silver bromide emulsion dispersed on a silica support has been studied in the CH_3OH/H_2O solution for H_2 evolution under UV illumination.[18] Also, AgBr was well-dispersed on an Al−MCM-41 support and was investigated as a visible light photocatalyst for the decomposition of acetaldehyde in the gas phase.[19] In these two reaction systems, AgBr shows high stability and photocatalytic activity. However, to date, there is no evidence nor reasonable explanation for these performances of AgBr.

In this paper, AgBr was dispersed on P-25 TiO_2 support by impregnating P-25 TiO_2 in the aqueous solution of $AgNO_3$ and NH_4OH containing cetylmethylammonium bromide. The visible light driven photocatalytic activity of Ag/AgBr/TiO_2 was investigated for the photocatalytic decomposition of azodyes and *Escherichia coli*. Electron spin resonance (ESR) was used to detect the reactive species involved in the reaction. In combination with X-ray diffractometry (XRD), X-ray photoelectron spectroscopy (XPS), and Auger electron spectroscopy (AES), the visible light photocatalytic mechanism of Ag/AgBr/TiO_2 and the mechanism of AgBr photostability were illustrated and confirmed for the first time.

2. Experimental Section

2.1. Materials. Titania P-25 (TiO_2; ca. 80% anatase, 20% rutile; BET area, ca. 50 $m^2\ g^{-1}$) was purchased from the Degussa Co. Spin trap 5,5-dimethyl-1-pyrroline-*N*-oxide (DMPO) was purchased from the Sigma Chemical Co. *Escherichia coli* (*E. coli*) was from the laboratory of the Biological Technology Group of Research Center for Eco-Environmental Sciences. Azodyes acid red B (ARB), reactive red K-2G (K-2G), cationic red X-GRL (CRX), and reactive brilliant red X-3B (X-3B) were kindly supplied by the Shanghai Chemical Co. and were used without further purification. All other chemicals were analytical grade. Deionized and doubly distilled water was used throughout this study.

2.2. Preparation of Catalysts. Ag/AgBr/TiO_2 were prepared by the deposition−precipitation method. A 1-g quantity of P-25 TiO_2 was added to 100 mL of distilled water, and the suspension was sonicated for 30 min. Then, 1.2 g of cetylmethylammonium bromide (CTAB) was added to the suspension, and the mixture was stirred magnetically for 30 min, then 0.21 g of $AgNO_3$ in 2.3 mL of NH_4OH (25 wt % NH_3) was quickly added to the mixture. In this process, at alkaline condition, cationic surfactant CTAB could adsorb onto the surface of TiO_2 to limit the number of nucleation sites for a AgBr metal island to grow, leading to homogeneously dispersed AgBr. Besides this, CTAB could supply bromide to precipitate Ag^+ in solution. The amount of bromide ion from CTAB is more than sufficient to precipitate AgBr from the added $AgNO_3$. The resulting suspensions were

* To whom correspondence should be addressed. Telephone: +86-10-62849171. Fax:+86-10-62923541. E-mail: huchun@rcees.ac.cn.

10.1021/jp0564400 CCC: $33.50
Published on Web 02/14/2006

stirred at room temperature for 12 h. Then, the amount of Ag^+ in the supernatant was measured by inductively coupled plasma optical emission spectrometry (ICP-OES) on an OPTIMA 2000 (Perkin Elmer Co.) instrument, confirming that Ag content of 10 wt % was incorporated in TiO_2. The product was filtered, washed with water, and dried at 70 °C. Finally, the powder was calcined in air at 500 °C for 3 h. The Brunauer−Emmett−Teller (BET) surface area of the sample was 22 $m^2\ g^{-1}$. As a reference, Ag/TiO_2 were prepared by a photocatalytic deposition method. P-25 TiO_2 (2.00 g), methanol (4 mL), 0.1 M $AgNO_3$ (3.8 mL), and NaCl (22.2 mg) were added to an aqueous solution (200 mL). The suspensions contained in a 400-mL Pyrex round-bottom flask were purged with a stream of nitrogen and irradiated with a 4-W black light lamp (major wavelength 365 nm) for 3 h. After illumination, the particulates were separated by filtration and washed with deionized water, then dried at 100 °C. The BET surface area of Ag/TiO_2 was 47 $m^2\ g^{-1}$.

2.3. Characterization of Catalysts. Powder X-ray diffraction of catalyst was recorded on a Scintag-XDS-2000 diffractometer with Cu Kα radiation ($\lambda = 1.540\ 59$ Å). UV−visible absorption spectra of the samples were recorded on a UV−vis spectrophotometer (Hitachi UV-3100) with an integrating sphere attachment. The analyzed range was 200−800 nm, and $BaSO_4$ was the reflectance standard. The XPS data were taken on an AXIS−Ultra instrument from Kratos using monochromatic Al Kα radiation (225 W, 15 mA, 15 kV) and low-energy electron flooding for charge compensation. To compensate for surface charges effects, binding energies were calibrated using the C1s hydrocarbon peak at 284.80 eV. AES measurements were performed on an AXIS−Ultra instrument from Kratos. The XPS and AES data were converted into the VAMAS file format and imported into the CasaXPS software package for manipulation and curve-fitting. Electron spin resonance (ESR) spectra were obtained using a Bruker model ESP 300 E electron paramagnetic resonance spectrometer equipped with a quanta-Ray Nd:YAG laser system as the irradiation light source ($\lambda = 532$ nm). The settings were center field, 3480.00 G; microwave frequency, 9.79 GHz; and power, 5.05 mW. Determination of the concentration of H_2O_2 formed in the catalyst aqueous suspension under visible light irradiation was performed with a photometric method described in the literature.[20]

2.4. Photocatalytic Degradation of Azodyes under Visible Light. The light source for photocatalysis was a 350-W Xe arc lamp (Shanghai Photoelectron Device Ltd.). Light passed through a water filter and a UV cutoff filter ($\lambda > 420$ nm) and then was focused onto a 100-mL beaker. The reaction temperature was maintained at 25 °C. Most of the azodyes are known to inhibit biological treatment of wastewater from the textile or dyeing industry.[21] Four non-biodegradable azodyes (ARB, K-2G, CRX, X-3B) were selected as model chemicals to evaluate the activity and properties of the catalyst. In a typical experiment, aqueous suspensions of azodyes (60 mL, 50 mg L^{-1}) and 100 mg of catalyst powders were placed in the beaker. Prior to irradiation, the suspensions were magnetically stirred in the dark for ca. 30 min to establish adsorption/desorption equilibrium between the dye and the surface of the catalyst under room air equilibrated conditions. At given irradiation time intervals, 3-mL aliquots were collected, centrifuged, and then filtered through a Millipore filter (pore size 0.22 μm) to remove the catalyst particulates for analysis. The filtrates were analyzed by recording variations at the wavelength of maximal absorption in the UV−vis spectra of dyes using model 752N spectrophotometer (Shanghai Precision & Scientific Instrument Co., Ltd., China). Total organic carbon of the solution was analyzed with the Apollo9000 TOC analyzer. The SO_4^{2-} ions were determined by ionic chromatography (Dionex Series 4500!).

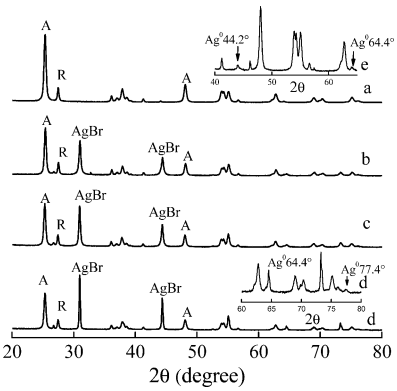

Figure 1. XRD pattern of (a) P-25 TiO_2, (b) fresh $Ag/AgBr/TiO_2$, (c) after photodegradation of ARB under visible light irradiation, (d) after UV irradiation for 60 h. The insert (d) shows peaks of Ag^0 in the structure of $Ag/AgBr/TiO_2$ after UV irradiation. The insert (e) shows XRD pattern of Ag/TiO_2 (A, anatase; R, rutile).

2.5. Bacterial Activity on $Ag/AgBr/TiO_2$. The bactericidal experiments were performed in an open round glass dish, with an illuminated area of 64 cm^2, under visible light as the above light source. The model bacteria *E. coli* belong to the waterborne pathogenic microorganisms. It was incubated in LB nutrient solution at 30 °C for 18 h with shaking, and then washed by centrifuging at 4000 rpm. The treated cells were then resuspended and diluted to $\sim 2 \times 10^7$ colony-forming units (CFU mL^{-1}) with 0.9% saline. The diluted cell suspension (30 mL) and 0.2 g L^{-1} $Ag/AgBr/TiO_2$ were added to the glass plate with a cover. Before and during light irradiation, an aliquot of the reaction solution was immediately diluted with saline, and an appropriate dilution of the sample was incubated at 37 °C for 24 h on nutrient agar medium, and then, the colonies were counted to determine the number of viable cells. For the measurement of K^+ leakage from the inactive *E. coli*, at every time interval, 1 mL of the illuminated bacterial suspension was centrifuged and the supernatant used for ICP-OES analysis. All of the above experiments were repeated three times.

2.6. Transmission Electron Microscopy (TEM). A quantity (10^8 CFU mL^{-1}) of cells was mixed with 0.2 g L^{-1} of $Ag/AgBr/TiO_2$, and the suspension was irradiated. At given time intervals, the cell suspension was collected and centrifuged down to a pellet. For the TEM analysis of *E. coli*, all samples were prepared according to the following standard procedures.[22] The bacteria pellets were pre-fixed in 2.5% glutaraldehyde at 4 °C for 12 h, then washed two times with 0.1 M phosphate buffer (PBS) (pH 7.2). After washing with PBS, the specimens were colored by mixing with 2% $Na_2H_5[P(W_2O_7)_6]$ aqueous solution at volume ratio 1:1 for 2 h. Then, the mixing suspension was dropped onto the cupper grids with holey carbon film. The grids were dried at natural condition and examined using a TEM Hitachi H-7500. The same experiments were repeated three times.

3. Results and Discussions

3.1. Characterization of Photocatalysts. Figure 1 shows the XRD patterns of the catalysts. The diffraction peaks attributed to AgBr were observed for three different $Ag/AgBr/TiO_2$ samples. All samples exhibited the common anatase and rutile phases of P-25 TiO_2. Beside this, the diffraction peaks (64.4°, 77.4°) assigned to Ag^0 were displayed in the sample of $Ag/AgBr/TiO_2$ irradiated by UV for 60 h, as depicted in the insert

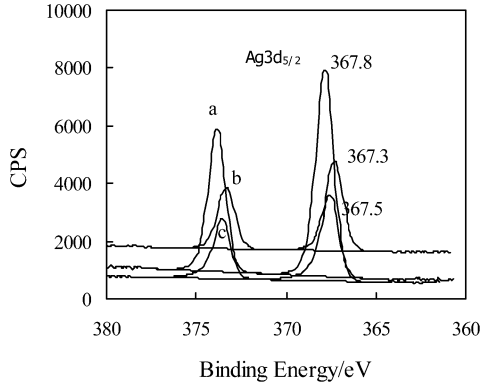

Figure 2. Ag 3d XPS spectra for (a) the fresh $Ag/AgBr/TiO_2$ and (b) after photodegradation of ARB under visible light irradiation and (c) Ag/TiO_2.

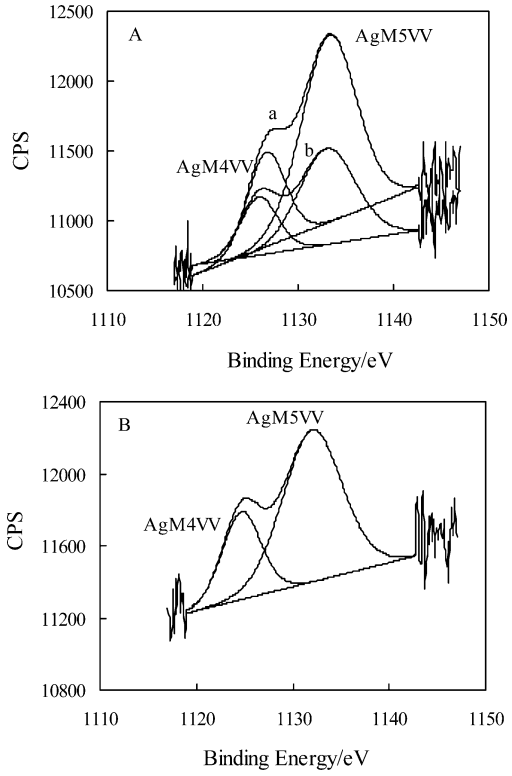

Figure 3. Ag AES spectra for (A) the $Ag/AgBr/TiO_2$ before (a) and after (b) photodegradation of ARB under visible light irradiation and (B) Ag/TiO_2.

(d) of Figure 1; while the peak at 64.4° appeared, another one at 77.4° did not in the fresh and used $Ag/AgBr/TiO_2$ in visible light reaction. The results indicated that Ag^0 species also possibly existed in the two samples. For Ag/TiO_2, two peaks $2\theta = 44.2°$, 64.4° assigned to Ag^0 significantly appeared in the insert (e) of Figure 1. To affirm the metallic state of the silver on the surface of these samples, the fresh and used $Ag/AgBr/TiO_2$ in visible light and the fresh Ag/TiO_2 were further characterized by XPS and AES measurements. Figures 2 and 3 showed the XPS and AES profiles of them. On the basis of the calculation of the Auger parameter (=BE ($Ag3d_{5/2}$) − Auger (M4VV) + 1486.71 (characteristic energy, eV)), the Auger parameters of the element Ag for the $Ag/AgBr/TiO_2$ before and after visible light reaction and Ag/TiO_2 were 726.25, 725.82, and 727.02 eV assigned to Ag^0,[23−25] respectively. The results confirm that the surface Ag species mainly exist as Ag^0 in all the $Ag/AgBr/TiO_2$ samples. On the basis of the above information, it is proposed that the Ag^0 formation occurred accompanying the formation of AgBr during the preparation of the catalyst. The concentrations of Ag^0, bromide ions, titanium, and oxygen on the surface of the fresh $Ag/AgBr/TiO_2$ were 3.41, 1.57, 23.52, and 54.05 at. %, respectively, by XPS analysis, indicating that the surface of TiO_2 was not completely covered by Ag^0 and AgBr species. Ag^0 is the predominant Ag species on the surface of Ag/TiO_2, and its concentration was 1.35 at. % based on XRD, XPS, and AES measurements. The UV−vis spectra of $Ag/AgBr/TiO_2$ (Figure 4) exhibit a visible light absorption band around 400−750 nm corresponding to the indirect band gap, whereas the absorption peak around 290 nm assigned to the direct band gap of AgBr was overlaid by the strong absorption peak at 277 nm of TiO_2. Ag/TiO_2 also has an absorption band at 400−700 nm. The absorption band should be assigned to surface plasmon absorption of silver, centered at 490−530 nm. The bigger metal particles resulted in the absorption band broadening.[26]

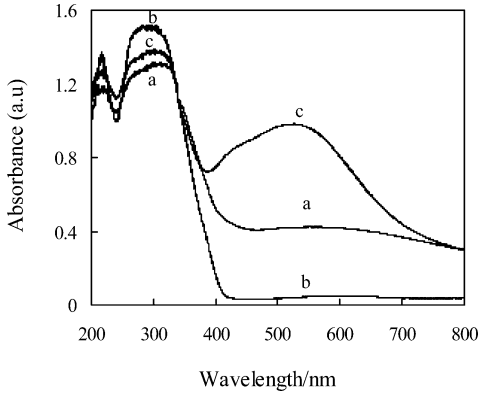

Figure 4. UV−vis diffuse reflectance spectra of (a) $Ag/AgBr/TiO_2$, (b) TiO_2, and (c) Ag/TiO_2.

3.2. Photodegradation of Azodyes under Visible Light Irradiation. Figure 5A shows photocatalytic degradation of azodye ARB under different visible light illuminated catalysts. As a comparison, ARB degradations over TiO_2 and Ag/TiO_2 were also performed under the same conditions and are shown in Figure 5A. Zhao and co-workers reported that many dyes could be degraded over TiO_2 on the basis of the self-photosensitization process of dyes under visible light irradiation.[27,28] However, a similar phenomenon did not occur in the degradation of ARB over TiO_2 and Ag/TiO_2 under visible light irradiation. The reaction of ARB photodegradation initiated by the light-excited dye was not observed in both cases. In contrast, $Ag/AgBr/TiO_2$ photocatalyst exhibited a high activity for ARB degradation under visible light ($\lambda > 420$ nm). These results indicated that the transformation of photoelectrons from the excited state of ARB to the CB of TiO_2 could be ignored under these experimental conditions, while the photocatalytic process was the predominant process. Moreover, Figure 5B also shows that the total organic carbon of the solution continuously decreased and the formation of SO_4^{2-} increased after the ARB was completely decolorized, verifying that the photocatalytic process occurred in the visible light illuminated $Ag/AgBr/TiO_2$ system. After illumination for 4.5 h, about 50% of the total sulfur content was converted into SO_4^{2-} ions, and 60% of TOC were removed, indicating that ARB had not only been decolorized but also mineralized efficiently under visible light irradiation. As shown in Figure 6, the azodyes K-2G, X-3B, and CRX were degraded efficiently in $Ag/AgBr/TiO_2$ suspension under visible light irradiation as ARB. K-2G and X-3B also were almost completely decolorized at 60 min of irradiation. To illustrate the mechanism of $Ag/AgBr/TiO_2$ visible lightphotocatalysis, the formation of H_2O_2 was determined in aqueous $Ag/AgBr/TiO_2$

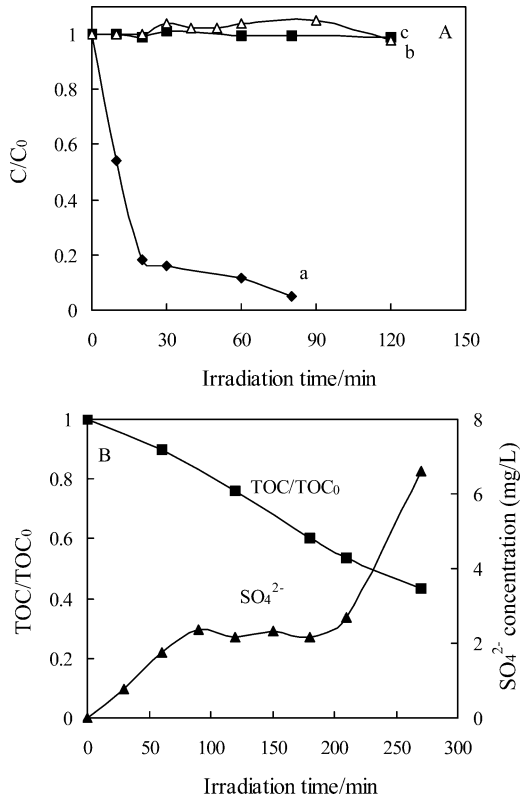

Figure 5. (A) Temporal course of the photodegradation of ARB (50 mg L^{-1}, 60 mL) in aqueous dispersions containing 0.1 g of catalysts under visible light irradiation: (a) $Ag/AgBr/TiO_2$, (b) TiO_2, and (c) Ag/TiO_2. (B) Formation of SO_4^{2-} and the removal of TOC during the degradation process in $Ag/AgBr/TiO_2$ system.

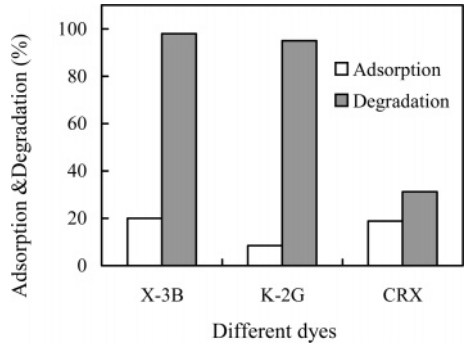

Figure 6. The adsorption and photodegradation of different azodyes (50 mg L^{-1}, 60 mL) in aqueous dispersions containing 0.1 g of $Ag/AgBr/TiO_2$ under visible light irradiation (irradiation time: 60 min).

and Ag/TiO_2 suspensions without dyes to remove the self-photosensitized contribution under visible light irradiation (Figure 7). In the $Ag/AgBr/TiO_2$ system, the quantities of H_2O_2 increased with irradiation time, reached a maximal value, and then gradually decreased to a certain value, and increased again. In the Ag/TiO_2 system, there was almost no H_2O_2 formation. According to the photocatalytic mechanism,[5,29,30] the H_2O_2 could be formed from these reactions of photogenerated electron and hole with adsorbed oxygen/water, where $O_2^{-\bullet}$ and $^{\bullet}OH$ were possibly involved. Therefore, the results indicated that $O_2^{-\bullet}$ and $^{\bullet}OH$ reactive species were produced in aqueous $Ag/AgBr/TiO_2$ suspension under visible light irradiation, whereas in aqueous Ag/TiO_2 suspension, these reactive species were not present. To ascertain the conjecture, the ESR spin−trap technique (with DMPO) was used to detect the nature of the reactive oxygen species generated on the surface of catalysts under visible irradiation. A Nd: YAG laser (λ = 532 nm) was employed to

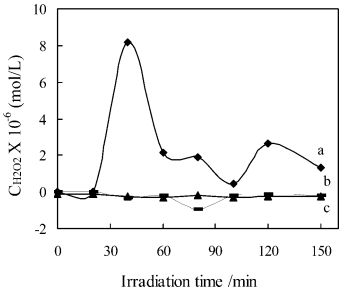

Figure 7. Plots showing the formation of H_2O_2 in aqueous dispersions containing 0.1 g of catalysts (a) $Ag/AgBr/TiO_2$ and (b) Ag/TiO_2 under visible light irradiation; (c) $Ag/AgBr/TiO_2$ in dark.

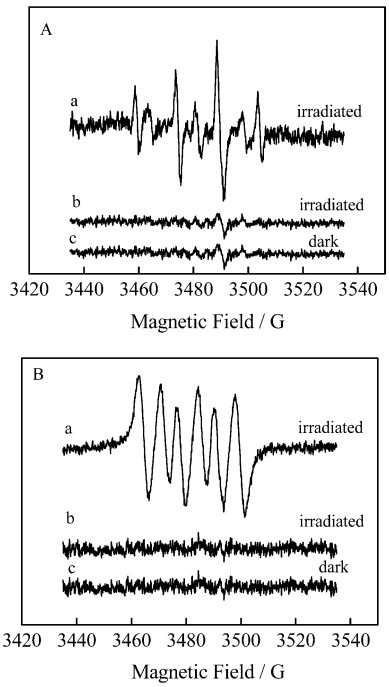

Figure 8. DMPO spin-trapping ESR spectra recorded at ambient temperature in aqueous dispersion (for DMPO-$^{\bullet}OH$, A) and methanol dispersion (for DMPO- $O_2^{\bullet-}$, B) under visible light irradiation (532 nm) (a) $Ag/AgBr/TiO_2$ and (b) Ag/TiO_2 under visible light irradiation; (c) $Ag/AgBr/TiO_2$ in dark.

irradiate catalyst aqueous suspensions without dye. Four characteristic peaks of DMPO-$^{\bullet}OH$ were observed in the suspension of $Ag/AgBr/TiO_2$ (Figure 8A). No such signals were detected in the dark. This means that irradiation is essential for the generation of $^{\bullet}OH$ on the surface of the catalyst. In contrast, no $^{\bullet}OH$ signals were detected in Ag/TiO_2 systems under the otherwise identical conditions. Similarly, the DMPO-$O_2^{-\bullet}$ species were detected successfully in $Ag/AgBr/TiO_2$ dipersions in methanolic media, since the $O_2^{-\bullet}$ radicals in water are very unstable and undergo facile disproportionation rather than slow reaction with DMPO.[31] The six characteristic peaks of the DMPO-$O_2^{-\bullet}$ adducts were observed only under visible light irradiation (Figure 8B). No such signals were detected in dark and visible light irradiated Ag/TiO_2 system. The evidence that $^{\bullet}OH$ and $O_2^{-\bullet}$ are produced on the surface of visible illuminated $Ag/AgBr/TiO_2$ provides a solid indication that the catalyst can be efficiently excited by visible light to create electron−hole pairs and that the charge separation is maintained long enough to react with adsorbed oxygen/H_2O and to produce a series of active oxygen radicals which finally decompose organic compounds as illustrated in previous work.[32,33] Neither $^{\bullet}OH$ nor $O_2^{-\bullet}$ was formed in the visible light illuminated Ag/TiO_2 suspension,

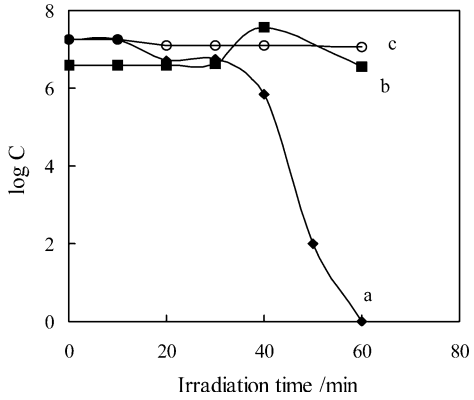

Figure 9. Temporal course of the *E. coli* inactivation (2×10^7, 30 mL) in aqueous dispersions containing 6 mg of catalysts (a) Ag/AgBr/TiO_2 and (b)TiO_2 under visible light irradiation; (c) Ag/AgBr/TiO_2 in dark.

indicating no reactive oxygen species generated from visible light excited plasmon resonance of Ag^0 metals on TiO_2, although Ag/TiO_2 has a strong absorption in the visible region. On the basis of all the information about reactive oxygen determination, we may deduce that, in the visible light illuminated Ag/AgBr/TiO_2 system, the mechanism of dye degradation is the mainly visible light driven photocatalytic process. AgBr deposited on TiO_2 is the active component and is responsible for the catalyst's visible light activity. AgBr can be excited by visible light and generate electron−hole pairs because of its absorption at 400−750 nm, while it is quite possible that Ag^0 species on the surface of Ag/AgBr/TiO_2 mainly act as electron traps, enhancing the electron−hole separation and the subsequent transfer of the trapped electron to the adsorbed O_2 acting as an electron acceptor according to the previous work.[15,34,35] To illustrate the visible light activity of AgBr, AgBr also was loaded on the SiO_2 by the same method as the preparation of Ag/AgBr/TiO_2. According to the previous work,[18] Ag^0 species also exist on the surface of AgBr/SiO_2 at the early stages of the preparation. The catalyst has an adsorption band at 400−600 nm beside the strong absorption peak around 290 nm. The catalyst also shows activity for the degradation of ARB under visible light irradiation, but its photocatalytic efficiency was lower than that of Ag/AgBr/TiO_2. The results indicated that AgBr is the main photoactive component and that the photocatalytic activity of AgBr was affected by different supports. Further experiments are necessary to understand the influence of the support on the photocatalytic activity of AgBr. On the other hand, the surface Ag^0 species play an important role for the stability of Ag/AgBr/TiO_2, which will be discussed further later in this paper.

3.3. Bactericidal Activity on Ag/AgBr/TiO_2 under Visible Light Irradiation. The bactericidal activities of the samples were evaluated by the inactivation of *E. coli* in water under visible light irradiation. As shown in Figure 9, *E. coli* was almost completely killed within 60 min in Ag/AgBr/TiO_2 under visible light irradiation. The complete *E. coli* inactivation of 7.2 log occurred at 60 min of irradiation. Neither pure TiO_2 nor Ag/AgBr/TiO_2 in the dark showed any bactericidal effects on *E. coli*, indicating that the photocatalyst itself is not toxic to *E. coli*. The inactivation of *E. coli* is mainly due to oxidative radicals ($^{\bullet}OH$, $O_2^{-\bullet}$, H_2O_2) produced by visible light irradiated Ag/AgBr/TiO_2. Furthermore, in this system, the changes of the morphology of *E. coli* for different times of irradiation were observed by TEM. Figure 10A shows the appearance of *E. coli* before reaction. Characteristics of the *E. coli* are the well-defined cell wall as well as the evenly colored interior of the cell, which corresponds to the presence of proteins and DNA. The morphology of *E. coli* illuminated for 30 min greatly changed (Figure 10B). Part of the cell wall was decomposed, and the colored interior of the cell became white, indicating that the outer membrane of the cell was damaged leading to a leakage of the interior component. This phenomenon was more significantly shown in the images of *E. coli* for 2 and 4 h irradiation (Figure 10C−E). With irradiation time increasing, the catalyst nanoparticles penetrated inside the cells, resulting in more damage to the membrane of the cell. The lipopolysaccharide layer of the outer membrane plays an essential role in providing a barrier of selective permeability for *E. coli* Gram-negative bacteria. On the basis of the TEM investigation, Ag/AgBr/TiO_2 photocatalyst could decompose the peptidoglycan layer and subsequently destroy the cell wall and the cell membrane, leading to a change in the cell membrane permeability and resultant leakage of intracellular substances. K^+ exists universally in bacteria[36] and plays roles in the regulation of polysome content and protein synthesis. Therefore, K^+ leakage from *E. coli* was used, in this work, to examine the permeability of the cell membrane. Figure 11 shows K^+ leakage with the inactivation of the *E. coli* in different visible light illuminated catalyst suspensions. In the visible light illuminated TiO_2 system and in dark Ag/AgBr/TiO_2 suspensions, there was almost no K^+ leakage from *E. coli* cells. Oppositely, in the visible light illuminated Ag/AgBr/TiO_2 suspension, K^+ immediately leaked out and promptly increased paralleling the inactivation of *E. coli* with irradiation time. Within 40 min, the inactivation of *E. coli* was not significant from Figure 9, but the concentration of K^+ ions were increasing drastically. According to the previous work,[37] the bactericidal activity consists of two steps: First, disordering of the outer membrane in the cell envelope occurs, followed by the disordering of the inner membrane. In the first step, there is K^+ leakage from *E. coli*, while *E. coli* is not inactivated at the same time. Thus, at the initial stage of the reaction, the inactivation of *E. coli* lagged the K^+ leakage. In the period of 60−90 min, the concentration of K^+ ions reached relatively steady values with increasing illumination time, and then further increased notably when illumination time increased to 120 min, because of the greater destruction of the cell membrane (shown in Figure 10C). The results demonstrate that the K^+ leakage was consistent with the decomposition of the cell wall and the cell membrane. These data demonstrate that the visible light bactericidal mechanism of Ag/AgBr/TiO_2 is similar to that of TiO_2 in UV illumination. The cell wall and the cell membrane were subsequently decomposed by various reactive species (e.g., $^{\bullet}OH$, $HO_2^{\bullet}$, H_2O_2), causing the cell death.

3.4. Role of Ag^0 in the Photostability of Ag/AgBr/TiO_2. The durability of Ag/AgBr/TiO_2 catalyst is shown in Figure 12 for the degradation of ARB under visible light and UV irradiation. Ag/AgBr/TiO_2 was easily recycled by simple filtration without any treatment in these experiments. The photocatalytic activity did not decrease significantly in the degradation ARB after eight successive cycles under visible irradiation (Figure 12A). Under UV irradiation, five repeated experiments also exhibited that catalyst activity was almost same for the degradation of ARB (Figure 12B). Even after the catalyst was irradiated by UV for 60 h, the catalyst activity was maintained effectively. The results demonstrated that Ag/AgBr/TiO_2 is an effective and stable catalyst under visible light and UV irradiation. It is very well-known in the photographic field that silver halides are rather easily decomposed by light

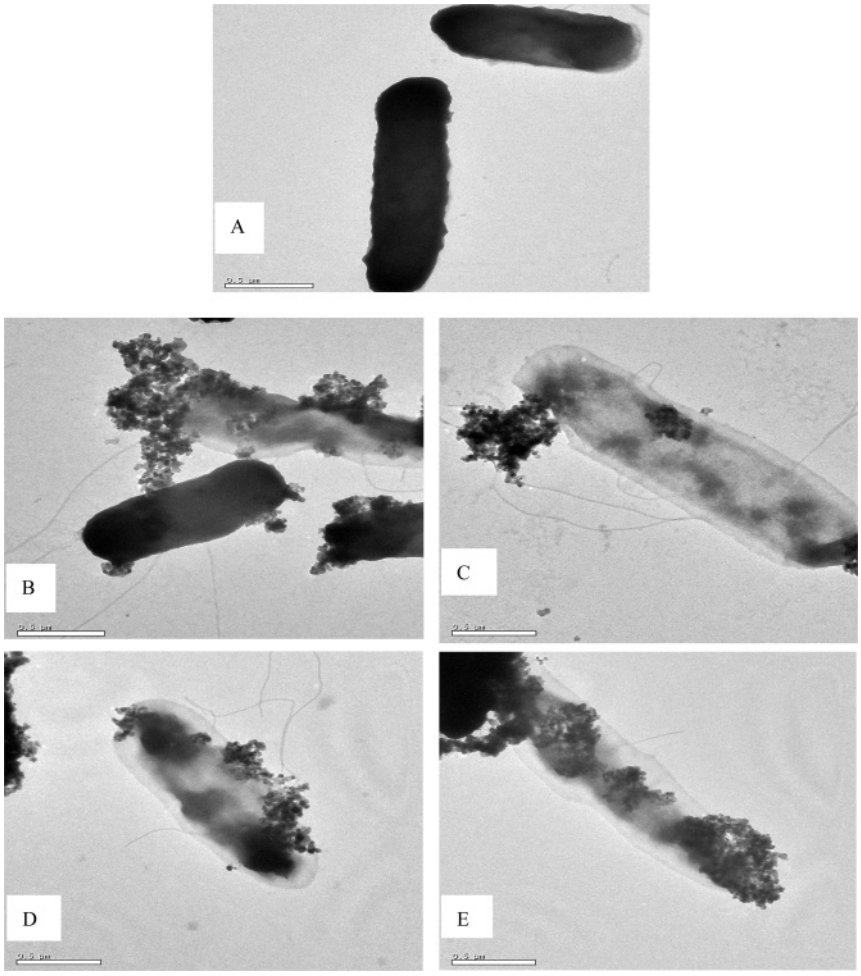

Figure 10. TEM images of *E. coli* for different reaction times in visible light illuminated Ag/AgBr/TiO_2 suspension: (A) *E. coli* before reaction, (B) *E. coli* treated for 0.5 h, (C) *E. coli* treated for 2 h, and (D) and (E) treated for 4h.

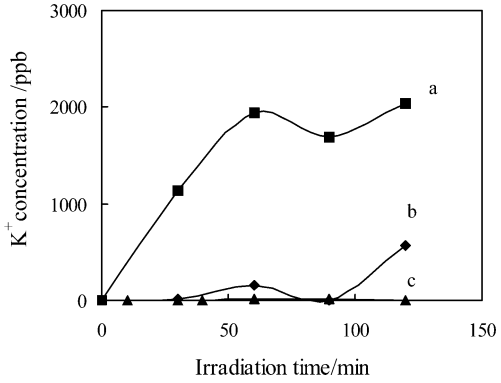

Figure 11. Leakage of K^+ ion from *E. coli* cells in aqueous dispersions containing 6 mg of catalysts (a) Ag/AgBr/TiO_2 and (b) TiO_2 under visible light irradiation; (c) Ag/AgBr/TiO_2 in dark.

absorption to form silver metals. It is very interesting why the Ag/AgBr/TiO_2 catalyst is so photostable. To elucidate the stable mechanism, the Ag/AgBr/TiO_2 sample irradiated by UV for 60 h and the other one after photocatalytic reaction under visible irradiation were characterized by XRD, XPS, and AES (Figures 1−3). In comparison with XRD patterns of the samples before and after irradiation, all the AgBr peaks became sharp after irradiation by UV or visible light, indicating the crystalline growth of AgBr. The results suggest that AgBr is not destroyed by exposure to visible light or UV. In addition, the peaks corresponding to Ag^0 appeared in XRD patterns of the sample after UV irradiation. Subsequently, it is also proved that Ag^0 mainly exists on the surface of the fresh and visible illuminated samples by XPS and AES measurements. Therefore, the Ag^0 formation occurred at the early stages of the catalyst preparation. It is possible that the formed Ag^0 species inhibit the decomposition of AgBr under visible light and UV. According to the studies of Agostiano et al.,[38] in the process of aerated photocatalysis, silver species mainly underwent the following reactions:

$$Ag^+ + e_{CB}^- \rightarrow Ag^0 \quad (1)$$

$$Ag^+ + R^\bullet \rightarrow Ag^0 + R' + H^+ \quad (2)$$

$$Ag^0 + h_{VB}^+ \rightarrow Ag^+ \quad (3)$$

where $R^\bullet$ referes to reactant radical. In the presence of oxygen, reaction 3 progressively becomes the dominant process, although hole scavenging by the reactant is beneficial toward reactions 1 and 2. The efficient e_{CB}^- scavenging by dissolved oxygen can result both in a decreased number of e_{CB}^- for Ag^+ photoreduction and in a higher availability of h_{VB}^+. Figure 2 shows that the XPS peak intensity of Ag^0 of Ag/AgBr/TiO_2 after photocatalytic reaction is lower than that before photocatalytic reaction, indicating that reaction 3 mainly occurred during the degradation of ARB under visible light. Therefore, the Ag^0 species on the surface of Ag/AgBr/TiO_2 is responsible for the catalyst stability under UV and visible light irradiation.

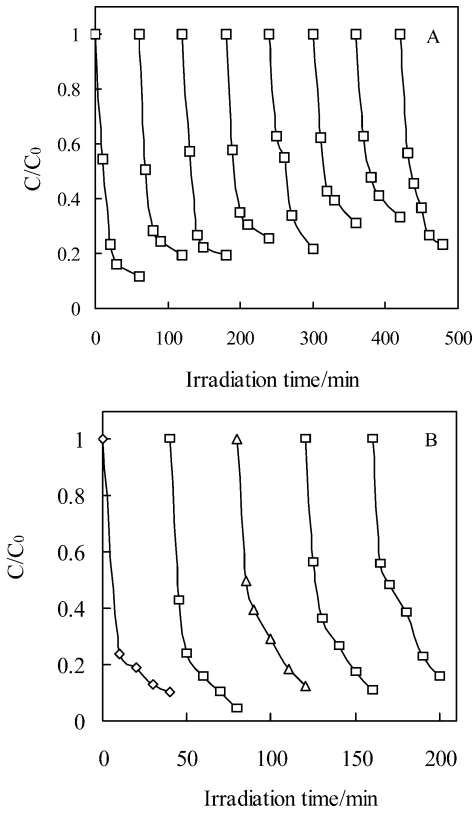

Figure 12. Cycling runs in the photodegradation of ARB in the presence of Ag/AgBr/TiO_2 under visible light (A) and UV (B) irradiation. Ag/AgBr/TiO_2 (1.6 g L^{-1}); addition of ARB (50 mg L^{-1} per run).

4. Conclusions

Ag/AgBr/TiO_2 was prepared by deposition−precipitation and was found to be a novel visible light driven photocatalyst for the degradation of dyes and inactivation of bacteria. The catalyst exhibits high photocatalytic activity, not only in the decolorization and mineralization of azodyes, but also in the inactivation of *E. coli* under visible light irradiation. The studies of ESR and H_2O_2 formation show that $^{\bullet}OH$ and $O_2^{-\bullet}$ were formed in aqueous Ag/AgBr/TiO_2 suspension under visible light irradiation, whereas there is no reactive oxygen species to occur in aqueous Ag/TiO_2 suspension under otherwise identical conditions. The evidence indicates that AgBr is the visible light active component of the catalyst and that Ag^0 species on the surface of the catalyst is possibly contributing to enhancing the electron−hole separation and interfacial charge transfer. Furthermore, the catalyst activity and crystal structure did not change after a series of repeated experiments for the degradation of ARB under different experimental conditions. The results of XRD, XPS, and AES demonstrate the mechanism of the catalyst photostability. The surface Ag^0 species scavenged h_{VB}^+ and then trapped electrons to inhibit the decomposition of AgBr. In addition, the results of bactericidal experiments under visible light irradiation verified that the cell wall and the cell membrane were successively decomposed by reactive oxygen species ($^{\bullet}OH$, $O_2^{\bullet-}$, H_2O_2), leading to the leakage of intracellular molecules and causing the cell death.

Acknowledgment. This work was supported by the National 863 Project of China (no. 2005AA642030) and the Natural Sciences Foundation of China (nos. 20577062, 20377050, 20537020, 50538090). We thank Dr. Chuncheng Chen (Institute of Chemistry, Chinese Academy of Sciences) for his valuable discussion about ESR studies.

Supporting Information Available: Additional spectra and degradation graphs. This material is available free of charge via the Internet at http://pubs.acs.org.

References and Notes

(1) Yu, J. C.; Ho, W.; Yu, J.; Yip, H.; Wong, P. K.; Zhao, J. *Environ. Sci. Technol.* **2005**, *39*, 1175.
(2) Wolfrum, E. J.; Huang, J.; Blake, D. M.; Maness, P.; Huang, Z.; Fiest, J. *Environ. Sci. Technol.* **2002**, *36*, 3412.
(3) Hu, C.; Yu, J. C.; Hao, Z.; Wong, P. K. *Appl. Catal., B* **2003**, *42*, 47.
(4) Kamat, P. V. *Chem. Rev.* **1993**, *93*, 267.
(5) Mills, A.; Hunte, S. Le. *J. Photochem. Photobiol., A* **1997**, *108*, 1.
(6) Choi, W.; Termin, A.; Hoffmann, M. R. *J. Phys. Chem.* **1994**, *98*, 13669.
(7) Asahi, R.; Morikawa, T.; Ohwaki, T.; Aoki, K.; Taga, Y. *Science* **2001**, *293*, 269.
(8) Zhao, W.; Ma, W.; Chen, C.; Zhao, J.; Shuai, Z. *J. Am. Chem. Soc.* **2004**, *126*, 4782.
(9) Sakthivel, S.; Kisch, H. *Angew. Chem., Int. Ed.* **2003**, *42*, 4908.
(10) Zhao, G.; Kozuka, H.; Yoko, T. *Thin Solid Films* **1996**, *277*, 147.
(11) Wang, C.-M.; Heller, A.; Gerischer, H. *J. Am. Chem. Soc.* **1992**, *114*, 5230.
(12) Driessen, M. D.; Grassian, V. H. *J. Phys. Chem. B* **1998**, *102*, 1418.
(13) Bae, E.; Coi, W. *Environ. Sci. Technol.* **2003**, *37*, 147.
(14) Arabatzis, I. M.; Stergiopoulos, T.; Bernard, M. C.; Labou, D.; Neophytides, S. G.; Falaras, P. *Appl. Catal., B* **2003**, *42*, 187.
(15) Zhao, W.; Chen, C.; Li, X.; Zhao, J. *J. Phys. Chem. B* **2002**, *106*, 5022.
(16) Fessenden, R. W.; Kamat, P. V. *J. Phys. Chem.* **1995**, *99*, 12902.
(17) Stipkala, J. M.; Castellano, F. N.; Heimer, T. A.; Kelly, C. A.; Livi, K. J. T.; Meyer, G. J. *Chem. Mater.* **1997**, *9*, 2341.
(18) Kakuta, N.; Goto, N.; Ohkita, H.; Mizushima, T. *J. Phys. Chem. B* **1999**, *103*, 5917.
(19) Rodrigues, S.; Uma, S.; Martyanov, I. N.; Klabunde, K. J. *J. Catal.* **2005**, *233*, 405.
(20) Bader, H.; Sturzenegger, V.; Hoigne, J. *Water Res.* **1988**, *22*, 1109.
(21) Martin, H. M. *Photodegradation of Water Pollutant*; CRC Press: Boca Raton, 1996.
(22) Shen, P.; Fan X.; Li, G. *Wei Sheng Wu Xue Shiyan*; High Education Publisher: Beijing, 2004.
(23) Schoen, G. *Acta Chem. Scand.* **1973**, *27*, 2623.
(24) Wagner, C. D. *Discuss. Faraday Soc.* **1975**, *60*, 291.
(25) Anthony, M. T.; Seah, M. P. *Surf. Interface Anal.* **1984**, *6*, 95.
(26) Kamat, P. V. *J. Phys. Chem. B* **2002**, *106*, 7729.
(27) Wu, T.; Liu, G.; Zhao, J.; Hidaka, H.; Serpone, N. *J. Phys. Chem. B* **1998**, *102*, 5845.
(28) Wu, T.; Liu, G.; Zhao, J.; Hidaka, H.; Serpone, N. *J. Phys. Chem. B* **1999**, *103*, 4862.
(29) Turchi, C. S.; Ollis, D. F. *J. Catal.* **1989**, *119*, 483.
(30) Hoffman, M. R.; Martin, S. T.; Choi, W.; Bahnemann, D. W. *Chem. Rev.* **1995**, *95*, 69.
(31) Ma, W.; Huang, Y.; Li, J.; Chen, M.; Song, W.; Zhao, J. *Chem. Commun.* **2003**, 1583.
(32) Maldotti, A.; Molinari, A.; Amadelli, R. *Chem. Rev.* **2002**, *102*, 3811 and references therein.
(33) Linsebigler, A. L.; Lu, G.; Yates, J. T. *Chem. Rev.* **1995**, *95*, 735 and references therein.
(34) Disdier, J.; Herrmenn, J. M.; Pichat, P. *J. Phys. Chem.* **1986**, *90*, 6028.
(35) Henglein, A. *J. Phys. Chem.* **1979**, *83*, 2209.
(36) Willis, D. B.; Ennis, H. L. *J. Bacteriol.* **1968**, *96*, 2035.
(37) Sunada, K.; Kikuchi, Y.; Hashimoto, K.; Fujishima, A. *Environ. Sci. Technol.* **1998**, *32*, 726.
(38) Cozzoli, P. D.; Comparelli, R.; Fanizza, E.; Curri, M. L.; Agostiano, A.; Laub, D. *J. Am. Chem. Soc.* **2004**, *126*, 386.